AD_____

Award Number: W81XWH-07-1-0516

TITLE: The Structural Basis of Pathogen Recognition by TLR Receptors of the Innate Immune System

PRINCIPAL INVESTIGATOR: Yorgo Modis, Ph.D.

CONTRACTING ORGANIZATION: Yale University
New Haven, CT 06520-8114

REPORT DATE: August 2008

TYPE OF REPORT: Final

PREPARED FOR: U.S. Army Medical Research and Materiel Command
Fort Detrick, Maryland 21702-5012

DISTRIBUTION STATEMENT: Approved for Public Release;
Distribution Unlimited

REPORT DOCUMENTATION PAGE

Form Approved
OMB No. 0704-0188

1. REPORT DATE	2. REPORT TYPE	3. DATES COVERED
01-Aug 2008	Final	16 Jul 2007 – 31 Jul 2008

4. TITLE AND SUBTITLE

The Structural Basis of Pathogen Recognition by TLR Receptors of the Innate Immune System

5a. CONTRACT NUMBER

5b. GRANT NUMBER
W81XWH-07-1-0516

5c. PROGRAM ELEMENT NUMBER

6. AUTHOR(S)

Yorgo Modis, Ph.D.

E-Mail: yorgo.modis@yale.edu

5d. PROJECT NUMBER

5e. TASK NUMBER

5f. WORK UNIT NUMBER

7. PERFORMING ORGANIZATION NAME(S) AND ADDRESS(ES)

Yale University
New Haven, CT 06520-8114

8. PERFORMING ORGANIZATION REPORT NUMBER

9. SPONSORING / MONITORING AGENCY NAME(S) AND ADDRESS(ES)
U.S. Army Medical Research and Materiel Command
Fort Detrick, Maryland 21702-5012

10. SPONSOR/MONITOR'S ACRONYM(S)

11. SPONSOR/MONITOR'S REPORT NUMBER(S)

12. DISTRIBUTION / AVAILABILITY STATEMENT
Approved for Public Release; Distribution Unlimited

13. SUPPLEMENTARY NOTES

14. ABSTRACT
The innate immune system is the first line of defense against invading pathogens. The overall goal of this project is to understand how a key family of innate immune receptors, the Toll-like receptors (TLRs), recognize their microbial ligands, and how this recognition is translated into an immune response. This report covers an initial one-year contract in a three-year project. In our first year, we developed methods to purify milligram quantities of TLR5, TLR11 and TLR12, and of their ligands, bacterial flagellin and Toxoplasma profilin (PFTG), respectively. We obtained crystals of TLR5, which diffract to 2.9-Å resolution, and crystals of PFTG, which diffract to 1.9 Å. We are currently pursuing the crystallographic structure determinations of TLR5 and PFTG. In parallel, we have obtained the first biochemical evidence for direct interaction between purified TLR5, TLR11 and flagellin. These results represent significant milestones towards our stated goal of understanding the molecular basis of pathogen recognition and signal generation by TLRs. Our work will guide efforts to design novel vaccine adjuvants.

15. SUBJECT TERMS
Innate immunity / toll-like receptor 5 / toll-like receptor 11 / toll-like receptor 12 / flagellin / profilin / vaccine design / adjuvant / protein crystallization

16. SECURITY CLASSIFICATION OF:			17. LIMITATION OF ABSTRACT	18. NUMBER OF PAGES	19a. NAME OF RESPONSIBLE PERSON
a. REPORT	b. ABSTRACT	c. THIS PAGE			USAMRMC
U	U	U	UU	21	19b. TELEPHONE NUMBER *(include area code)*

Table of Contents

INTRODUCTION

We rely on our innate immune system as the first line of defense response against invading pathogens. This immune response is critically dependent on the Toll-like receptors (TLRs). Each TLR recognizes a different molecular pattern that is characteristic of specific pathogens, such as bacterial cell wall components, bacterial filaments, or viral DNA and RNA. Upon ligand binding, TLRs transmit a signal to the nucleus that leads to the production of proinflammatory compounds. These include antimicrobial cytokines, and compounds that recruit the adaptive immune system, which establishes long-term immunity to specific pathogens. In this project, we aim to determine three-dimensional structures of human TLR5, TLR8 or TLR9, in complex with their ligands– bacterial flagellin, single-stranded RNA or CpG DNA, respectively. During the first year of research, we refined this aim to the structure determination of TLR5 in complex with its binding partner TLR11 and their common ligand bacterial flagellin, and we made significant progress towards this aim by obtaining high-quality crystals of TLR5. However, as stated in the original proposal application and in the award contract, this project was conceived and funded with the understanding that the research would take three years to complete. The results presented in this report therefore cover only the first year of a three-year research project, and, as expected, several of our research objectives still remain to be completed. A key research objective for the second and third years is to obtain the atomic structure of the TLR5-TLR11-flagellin complex, which will allow us to formulate a mechanistic hypothesis for the molecular basis of pathogen recognition and proinflammatory signal generation. To test our structure-based hypothesis on TLR5/TLR11 function, we will measure the effect on immune signaling of engineered mutations that are predicted from the structures to interfere with ligand binding or signal generation. We will also seek high-affinity TLR ligands, or agonists. Our work will reveal the molecular basis for how pathogen recognition is translated into an immune response signal. Our structure will guide efforts to design synthetic TLR agonists, which could serve as novel vaccine adjuvants, or as immunomodulatory therapeutics. Such therapeutics would provide a powerful new means to prevent and treat infectious diseases.

BODY

The overall goal of this project is to understand how Toll-like receptors (TLRs) recognize their natural ligands, and how the conformational changes induced upon ligand binding are translated into an inflammatory signal. The key objective in our original proposal was to determine the three-dimensional structure of a TLR alone and in complex with its ligand. Capturing the receptor-ligand interface in atomic detail will provide a powerful design platform for the generation of more specific and less toxic immunomodulatory therapeutics.

1. Overview of research accomplishments

In the first quarter of this three-year project, we established protocols for the routine production of one of the TLR-ligand pairs named as candidate components in our original proposal, namely the ***ectodomain of TLR5*** and its ligand, bacterial ***FliC flagellin***. Both proteins are stable and soluble, and can readily be purified in milligram quantities. This milestone corresponds to Aim 1a in our original proposal. Additionally, we have been able to express and purify ***full-length TLR5*** solubilized in detergent for use as a complementary reagent to the TLR ectodomain in ligand binding studies (Aim 1a) and in candidate agonist binding studies (Aim 3c in our proposal). Most notably, ***we obtained crystals of the TLR5 ectodomain***, which diffract at up to 2.8 Å resolution (part of Aim 1b). As a first step towards structure determination of TLR5 (part of Aim 1c), we collected several native and potential heavy metal derivative ***crystallographic datasets*** at synchrotron facilities.

In the second quarter, we collected several additional crystallographic datasets from our TLR5 ectodomain crystals at synchrotron facilities at Argonne National Laboratory. These datasets significantly advanced progress towards our stated aim to determine the three-dimensional structure of TLR5 (the first part of Aim 1c). We also learned from our collaborator Prof. Sankar Ghosh (Yale Department of Immunobiology) that ***TLR11 acts as a co-receptor with TLR5 for the recognition of bacterial flagellin.*** Similarly, we learned that ***TLR11 and TLR12 jointly recognize a protozoan profilin-like protein from the parasite Toxoplasma gondii (PFTG)*** (Sankar Ghosh, personal communication). In light of this new data, we refined our research aims so that instead of seeking crystals of the TLR5-FliC complex we are now seeking crystals of the TLR5-TLR11 complex and of the TLR5-TLR11-FliC ternary complex. In parallel, we decided to express and purify TLR12 and PFTG and assay for the formation of a TLR11-TLR12-PFTG complex. This provides an attractive alternative and/or complement to our work on the recognition of FliC by TLR5/TLR11. In pursuit of these refined aims, we ***established protocols for the routine production of milligram quantities of the ectodomain of TLR11 and of PFTG****.* Both proteins are stable and soluble, and can readily be purified in milligram quantities. This milestone is an alternative to Aim 1a in our original proposal. We also ***obtained crystals of PFTG****.*

In the third quarter, we continued to work towards the structure determination of the TLR5 ectodomain (TLR5-ECD). We collected additional crystallographic data and performed additional calculations in attempts to obtain the phases required for structure determination using various crystallographic methods. We ***set up extensive crystallization trials of TLR11-ECD****.* We clearly ***showed that TLR5-ECD alone does not bind FliC flagellin***, using various biochemical assays. We ***collected a complete crystallographic dataset from our crystals of PFTG****,* and initiated computational work in attempts to determine the structure of PFTG, which will be useful for the structure determination of the TLR11-TLR12-PFTG complex (an alternative to the second part of Aim 1c).

In the fourth quarter, we ***obtained an improved crystal form of PFTG, which diffracted to 1.9 Å resolution****.* We continued computational work towards the structure determinations of TLR5-ECD and PFTG. Finally, using our purified TLR5-ECD, TLR11-ECD and FliC material, we ***obtained the first biochemical evidence that TLR5-ECD, TLR11-ECD and FliC can form a ternary complex in vitro, in the absence of other proteins or cofactors****.*

2. Expression and purification of the ectodomain of mouse TLR5

TLRs have generally proven difficult to express in the quantities and quality necessary for structural studies. Nevertheless, we have developed a procedure to purify milligram quantities of the TLR5 ectodomain (outlined below), from which we were able to obtain high-quality crystals. We are encouraged by recent studies reporting the crystal structures of the TLR3 (Bell et al., 2005; Choe et al., 2005) and TLR4 ectodomains (Kim et al., 2007). Because the ligands of these TLRs are absent from both crystal structures, however, the molecular basis of recognition and innate immune signal generation by TLRs remains unknown.

Because TLR ectodomains are heavily glycosylated and contain multiple disulfide bridges, they must be expressed in a eukaryotic expression system. We chose the baculovirus-based insect cell expression system for its reproducibility, scaleability, and the sensitivity of insect glycans to endoglycosidases. The 80-kDa ectodomain of mouse TLR5 (TLR5-ECD) was cloned into the pAcGP67 vector (BD biosciences) with a histidine purification tag. Sf9 insect cells were co-transfected with the TLR5-ECD pAcGP67 expression construct and BaculoGold DNA (Sigma) to produce recombinant baculovirus. Sf9 or Hi5 insect cell infected with this virus overexpressed TLR5-ECD. Soluble TLR5-ECD was extracted from the cell lysate and loaded onto a nickel-affinity HisTrap column (GE Healthcare). The elution fractions were then

exchanged into a low salt buffer and loaded onto a MonoQ anion exchange column for further purification. Pure TLR5-ECD was obtained after size exclusion chromatography on a Superdex S200 column (see Figure 1). The low elution volume from the size exclusion column suggests that TLR5-ECD is most likely a trimer, a dimer or a tetramer in solution (in order of likelihood). As is evident from SDS-PAGE, the TLR5-ECD purified with this protocol contains various degrees of glycosylation ranging from no glycosylation (lower band) to the 16 kDa of glycans expected for the fully glycosylated ectodomain with 8 glycans (top band; see Figure 1). The glycans can be fully trimmed to just one N-acetyl-glucosamine side chain (and in most cases an α1,6-linked fucose) by treatment with endoglycosidase H. This procedure typically yields 0.6-1.0 mg of pure TLR5-ECD per liter of insect cell culture.

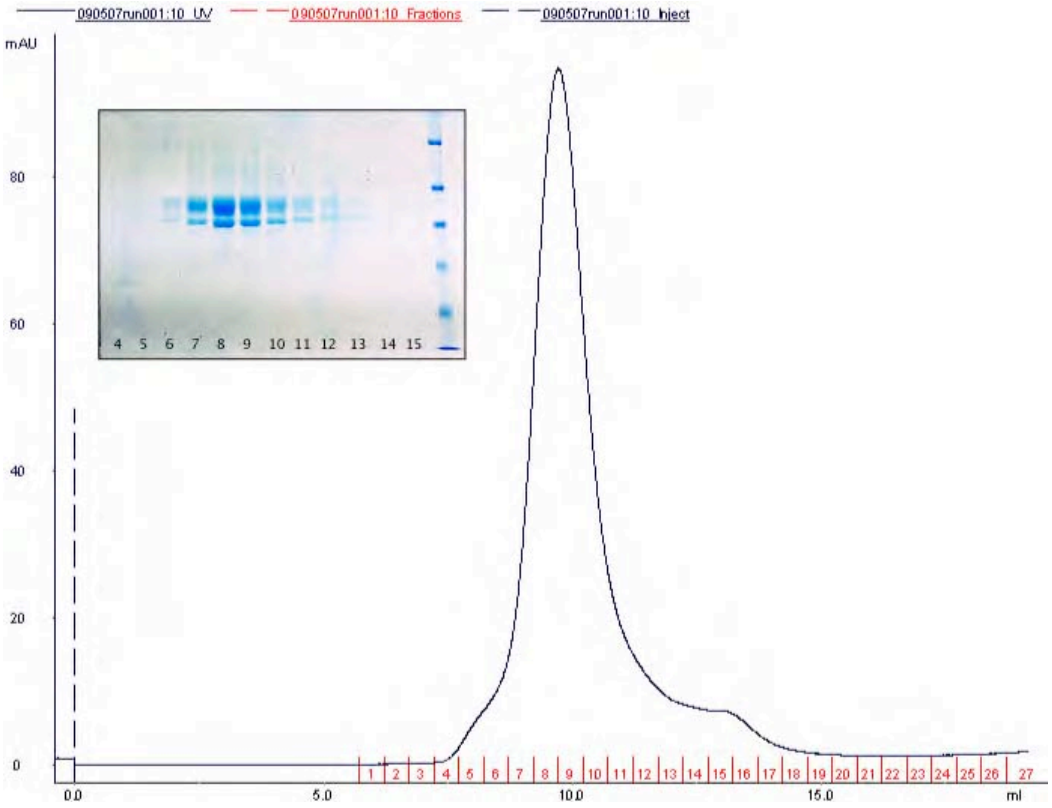

Fig. 1. Size exclusion chromatogram of TLR5 ectodomain (TLR-ECD) previously purified by nickel-affinity chromatography from insect cells. TLR5-ECD elutes at 9.68 ml. The oligomeric state of TLR5-ECD cannot be determined precisely from this chromatogram, given the expected highly elongated shape of TLR5-ECD, however the most likely oligomeric states are trimer, dimer and tetramer (in that order). Inset: Coomassie-stained SDS-PAGE gel showing pure TLR5-ECD in the peak fractions. On treatment with endoglycosidase H, the upper bands shift downwards by up to 16 kDa, merging with the lower band. This indicates that the upper bands are TLR5-ECD with different degrees of glycosylation, while the lower band is non-glycosylated protein.

3. Expression and purification of FliC flagellin from Salmonella typhimurium

Endogenous wild type FliC flagellin was purified from Salmonella typhimurium strain SJW1103. The first steps of our protocol are based on a previously established procedure in which the flagellar filaments are depolimerized with a heat treatment to yield monomeric flagellin (Silva-Herzog and Dreyfus, 1999). Briefly, cells were cultured overnight in LB media and harvested by centrifugation at 10,000 g for 20 min. The cell pellet was resuspended in 150 mM NaCl, 10 mM

triethanolamine pH 8.0, and 1 mM EDTA (Buffer A) and the flagellar filaments composed of FliC were detached from the cell bodies by vortexing. After removing contaminating aggregates and the cell bodies by centrifugation at 12,000 g, the flagellar filaments were collected by ultracentrifugation at 60,000 g for 1.5 h. The pellet was resuspended in Buffer A and flagellar filaments were depolymerized to monomeric FliC by heating at 60 ˚C for 5 min. After a short spin to remove aggregated materials, the supernatant was loaded onto a MonoQ anion exchange column (GE Healthcare). FliC in the elution fractions was further purified by size exclusion chromatography on a Superdex S200 column (GE Healthcare). This procedure reproducibly yields 10-12 mg of highly pure monomeric FliC per liter of cell culture. A typical size exclusion chromatogram with the corresponding SDS-PAGE gel is shown in Figure 2.

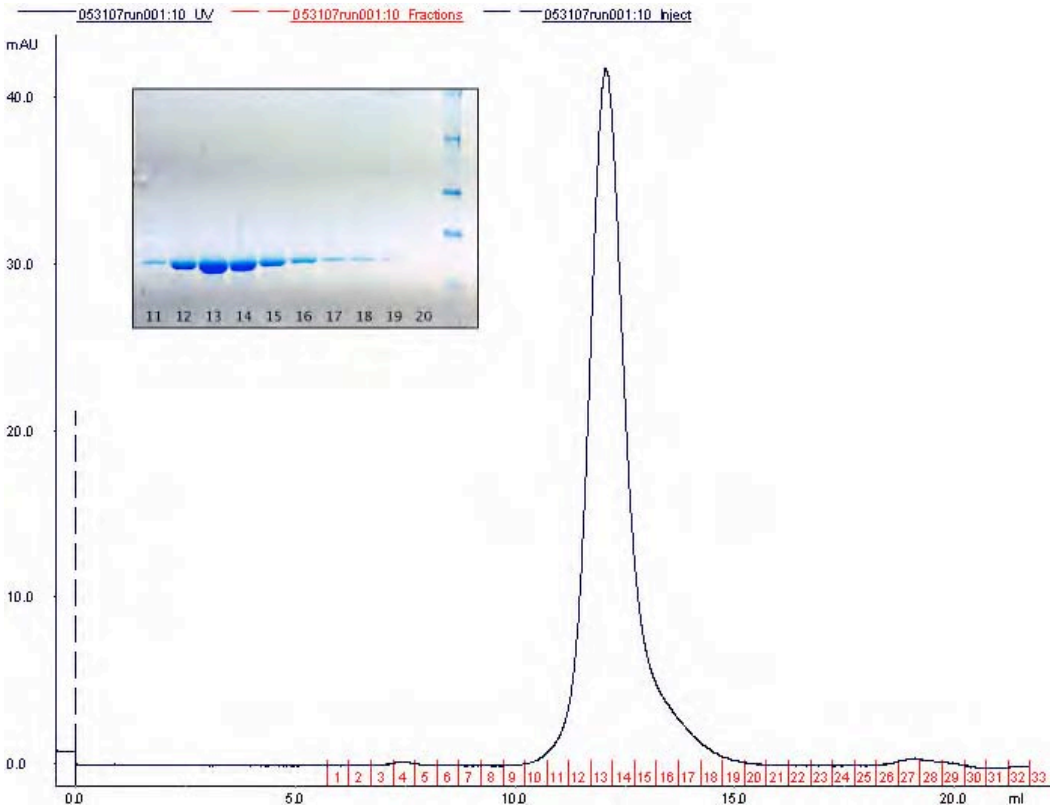

Fig. 2. Size exclusion chromatogram of endogenous wild type FliC flagellin from S. typhimurium previously purified by ion exchange chromatography. FliC elutes at 12.05 ml, which corresponds to an apparent size consistent with that of an elongated 55-kDa FliC monomer. Inset: Coomassie-stained SDS-PAGE gel showing pure FliC in the peak fractions.

4. Expression and purification of full-length human TLR5

In addition to measuring the binding affinity of flagellin and of candidate inhibitors for the TLR5 ectodomain, we plan to measure the binding affinities of those ligands for full-length TLR5 reconstituted into the lipid membrane of artificial liposomes (Aim 3c). Using full-length TLR5 will allow us to test whether the proximity of a lipid membrane and the presence of the TIR signaling domain contribute to ligand binding or receptor oligomerization. In pursuit of these aims, we have established a protocol to purify full-length TLR5, outlined below.

Full-length human TLR5 (FL-TLR5) was cloned into the pAcGP67 vector with a histidine purification tag. Sf9 insect cells were co-transfected with the FL-TLR5 pAcGP67 expression construct and baculoviral genomic DNA to produce recombinant baculovirus. Sf9 or Hi5 insect

cell infected with this virus over-expressed FL-TLR5 as a 100-kDa integral membrane protein. After cell lysis by sonication, the membrane fraction was separated by centrifugation at 100,000 g for 1 h. FL-TLR5 was extracted from the pellet with detergent before a second centriguation step. Solubilized FL-TLR5 was then partially purified from the supernatant by nickel-affinity chromatography. Optionally, the glycans could be removed from FL-TLR5 with endoglycosidase H. The protein was then purified to homogeneity by MonoQ ion exchange and size exclusion chromatography. This procedure typically yields 4 mg of pure FL-TLR5 per liter of insect cell culture. A typical size exclusion chromatogram with the corresponding SDS-PAGE gel is shown in Figure 3.

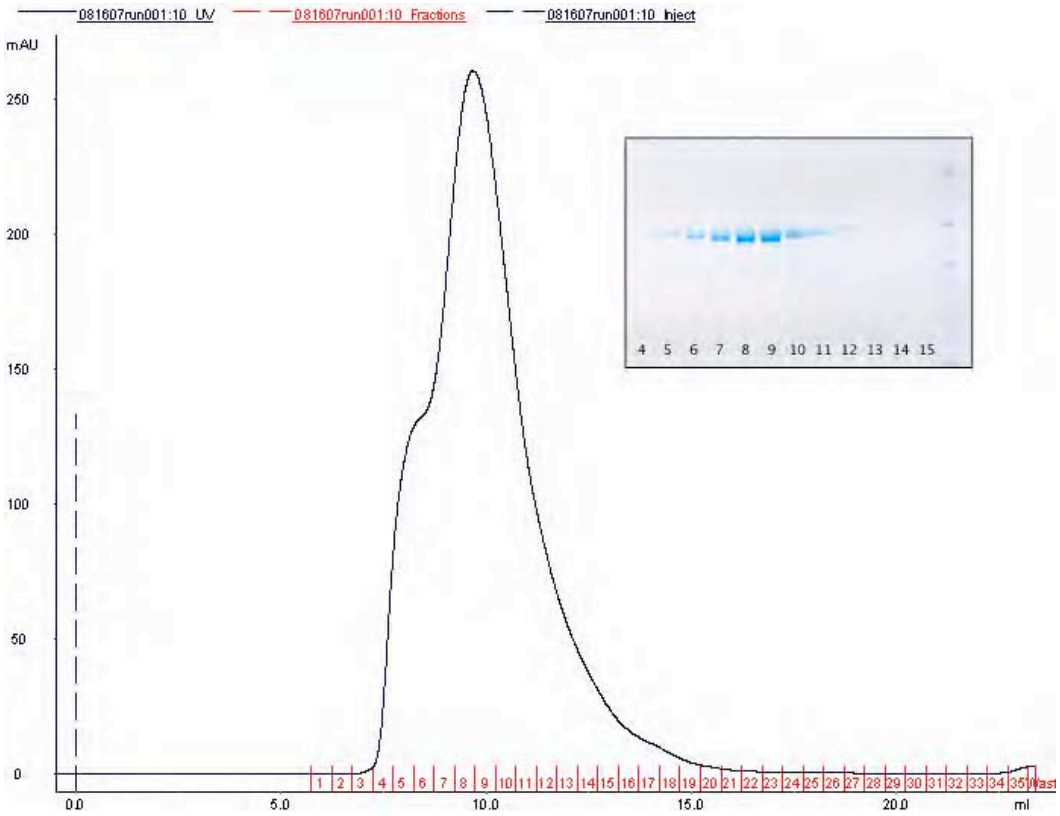

Fig. 3. Size exclusion chromatogram of deglycosylated full-length human TLR5 (FL-TLR5) previously purified from insect cell lysate by nickel-affinity chromatography. Most of the FL-TLR5 elutes as a soluble trimer, dimer or tetramer, at 9.69 ml elution volume. However, a significant fraction of the protein forms large aggregates and elutes in the void volume, producing a shoulder before the main peak. Inset: Coomassie-stained SDS-PAGE gel showing pure FL-TLR5 in the peak fractions. Some of the aggregated FL-TLR5 tends to precipitate or smear at the top of the gel (not shown).

5. Crystallization of the TLR5 ectodomain

With our automated robotic liquid handling system (Hydra II Plus One, Matrix Technologies) we were able to perform crystallization trials on our TLR5-ECD material using a large number of custom-made and commercially available precipitant solutions (QIAgen, Hampton Research). We recently obtained two distinct crystal forms of TLR5-ECD, under two different crystallization conditions. Both crystal forms were obtained using the vapor diffusion method, in both the hanging drop and sitting drop variations. Crystals of both crystal forms are small, with similar typical dimensions of approximately 40 x 30 x 20 µm. Diffraction images of the crystals taken at

state-of-the-art synchrotron X-ray sources showed sharp, isotropic diffraction at up to 2.8 Å resolution for the first crystal form, and 2.7 Å resolution for the second crystal form (Figure 4).

6. Crystallographic data collection for the TLR5 ectodomain

Crystallographic analysis of the data indicated that the first crystal form belonged to the high-symmetry cubic space group P4232, while the second crystal form belonged to space group C2. Due to the small size of the crystals, radiation damage had a pronounced effect on data quality as the diffraction experiment progressed, making it difficult to collect complete data beyond 3 Å resolution. A single P4232 crystal is sufficient, however, to collect a complete dataset at 3.3 Å resolution (see Table I). Moreover, many crystals are isomorphous as judged from their cell dimensions and merging R-factors, which allows data from more than one crystal to be combined to improve the quality of the dataset (see Table I). To date, we have collected native datasets from 20 crystals and potential heavy metal derivative datasets from 13 crystals soaked in one of the following heavy metal compounds: platinum tetrachloride, platinum hexachloride, ethyl mercury phosphate, ytterbium chloride and para-chloromercuri-phenylsulfonate (each at 1 mM). Data collection statistics for a representative candidate derivative dataset are shown in Table I. We are currently performing phasing calculations to determine the structure of the TLR5 ectodomain either by multiple isomorphous replacement, or by molecular replacement using the ectodomains of TLR3 or TLR4 as search models. Statistics for additional representative datasets are shown in Tables II and III.

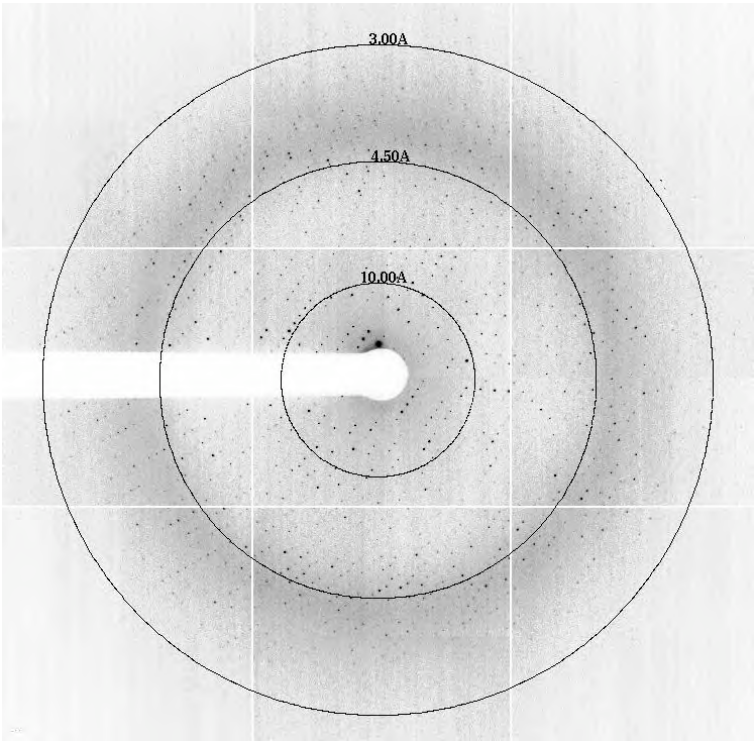

Fig. 4. X-ray diffraction pattern of a native crystal of the TLR5 ectodomain. The diffraction limit is 2.7 Å. This image was produced by a crystal belonging to space group C2 (see Table I, “Crystal Form 2”, for data collection statistics). Typical dimensions for these crystals are 40 x 30 x 20 µm. This image was recorded at the new 24-ID-E microfocus undulator beamline of the Northeastern Collaborative Access Team (NE-CAT) at the Advanced Photon Source, Argonne National Laboratory.

Table I. Data collection statistics for selected TLR5 ectodomain datasets. The "Crystal Form 1" and "Mercury Derivative" datasets were each collected from a single crystal. Data from three crystals were merged to produce the "Crystal Form 2" dataset. Both crystal forms diffract to better than 2.8 Å resolution, but because of the small size of the crystals (and the associated radiation damage), data between 2.7 Å and 3.19 Å resolution are incomplete and have been omitted from this analysis. The Mercury Derivative dataset belongs to Crystal Form 2.

Dataset	**Crystal Form 1**	**Crystal Form 2**	**Mercury Derivative**
Type of dataset	Native	Native	Derivative
Space group	*$P4_232$*	*C2*	*C2*
Cell dimensions: *a*, *b*, *c* (Å)	155.6, 155.6, 155.6	204.4, 146.5, 207.4	205.0, 147.2, 208.7
α, β, γ (°)	90, 90, 90	90, 92.9, 90	90, 93.1, 90
Resolution* (Å)	30-3.32 (3.44-3.32)	50-3.19 (3.39-3.19)	50-4.08 (4.27-4.08)
R_{merge}*	0.220 (0.496)	0.347 (0.653)	0.216 (0.673)
$I / \sigma I$	8.25 (2.16)	11.1 (1.94)	3.63 (1.37)
Completeness* (%)	97.1 (83.8)	99.3 (97.9)	72.3 (62.0)
Redundancy*	6.0 (2.8)	4.8 (3.1)	2.3 (1.8)
Number of molecules per asymmetric unit	1	~9	~9
Solvent content (%)	44	~50	~50

Table II. Data collection statistics for selected TLR5 ectodomain datasets collected in the current quarter. All datasets are in the high-symmetry cubic *$P4_232$* space group and were collected in December 2007 at Brookhaven National Laboratory.

Dataset name	**nai1**	**32Pt**	**33Ir**	**35Hg**	**nai3**
Compound soaked in	None	$K_2Pt(CN)_4$	$K_2Ir(CN)_6$	HgI_2	NaI (1 M)
Cell dimensions *a* = *b* = *c* (Å)	155.6	157.2	156.0	157.0	156.3
Resolution* (Å)	40 - 3.1	50 - 3.9	50 - 3.1	50 - 3.9	30 - 3.3
R_{merge}*	0.22 (0.46)	0.28 (0.64)	0.25 (0.73)	0.39 (1.00)	0.20 (0.38)
$I / \sigma I$	7.93 (1.18)	10.72 (3.25)	13.33 (2.09)	4.91 (1.09)	10.73 (3.19)
Completeness* (%)	97.1 (83.8)	98.8 (95.4)	98.8 (89.7)	93.4 (87.3)	99.5 (99.5)
Redundancy*	6.5 (1.1)	10.1 (5.9)	14.0 (5.0)	8.7 (4.1)	7.3 (3.6)
Number of molecules per asymmetric unit	1	1	1	~9	~9
Solvent content (%)	44	44	44	~50	~50

Table III. Data collection statistics for the TLR5-ECD datasets collected in the current quarter. The datasets were collected on April 16-17, 2008 at Argonne National Laboratory. *Numbers in parentheses refer to the highest resolution shell.

Dataset name	**M5ECD**	**5_5_1**	**nai2**	**32Pt**	**nai4**
Compound soaked in	None	$YbSO_4$	None	$K_2Pt(CN)_4$	NaI (1 M)
Cell dimensions *a*, *b*, *c* (Å)	204, 146, 207	206, 148, 210	156, 156, 156	157, 157, 157	156, 156, 156
Space group	*C2*	*C2*	$P4_232$	$P4_232$	$P4_232$
Resolution* (Å)	30 – 3.1	40 – 6.7	40 – 3.2	50 – 3.9	30 – 3.4
R_{merge}*	0.17 (0.40)	0.20 (0.70)	0.23 (0.50)	0.28 (0.64)	0.30 (0.48)
$I / \sigma I$	6.75 (1.7)	4.37 (1.0)	7.50 (1.38)	10.72 (3.25)	6.03 (2.63)
Completeness* (%)	72 (18.5)	67.1 (36.7)	92.9 (46.8)	98.8 (95.4)	98.2 (88.9)
Redundancy*	2.6 (1.2)	NA	6.4 (1.4)	10.1 (5.9)	6.5 (3.0)
Number of molecules per asymmetric unit	9	9	1	1	1
Solvent content (%)	50	50	44	44	44

7. Expression and purification of the ectodomain of mouse TLR11

For the expression of TLR11-ECD, we chose the same baculovirus-based insect cell expression system as we used for the expression of TLR5-ECD. The 80-kDa ectodomain of mouse TLR11 (TLR11-ECD) was cloned into the pAcGP67 vector (BD biosciences) with a histidine purification tag. Sf9 insect cells were co-transfected with the TLR11-ECD pAcGP67 expression construct and BaculoGold DNA (Sigma) to produce recombinant baculovirus. Sf9 or Hi5 insect cell infected with this virus overexpressed TLR11-ECD. Soluble TLR11-ECD was extracted from the cell lysate and loaded onto a nickel-affinity HisTrap column (GE Healthcare). The elution fractions were then loaded onto a Superdex S200 column for further purification of the TLR11-ECD (see Figure 5). As for TLR5-ECD, the low elution volume from the size exclusion column suggests that TLR11-ECD is most likely a trimer, a dimer or a tetramer in solution (in order of likelihood). As is evident from SDS-PAGE, the TLR11-ECD purified with this protocol contains various degrees of glycosylation ranging from no glycosylation (lower band) to the 8 kDa of glycans expected for the fully glycosylated ectodomain with 4 glycans (top band; see Figure 5). The glycans can be fully trimmed to just one N-acetyl-glucosamine side chain (and in most cases an α1,6-linked fucose) by treatment with endoglycosidase H. This procedure typically yields 1-1.5 mg of pure TLR11-ECD per liter of insect cell culture, almost twice as much protein as for TLR5-ECD.

We are currently working to optimize the above protocol to improve the level of purity and conformational homogeneity of purified TLR11, as judged from the SDS-PAGE and size exclusion chromatogram, respectively. Our strategy is to introduce an anion exchange chromatography step (MonoQ), as we did previously for TLR5-ECD.

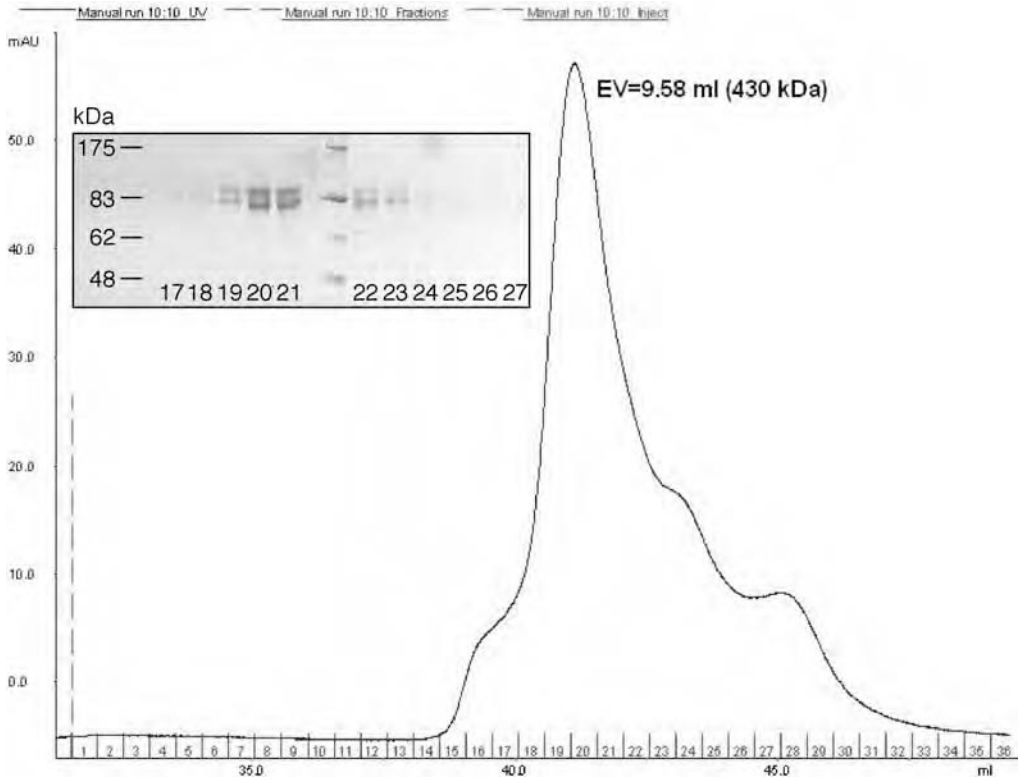

Fig. 5. Size exclusion chromatogram of TLR11 ectodomain (TLR-ECD) previously purified by nickel-affinity chromatography from insect cells. TLR11-ECD elutes at 9.58 ml. The oligomeric state of TLR11-ECD cannot be determined precisely from this chromatogram, given the expected highly elongated shape of TLR11-ECD, however the most likely oligomeric states are trimer, dimer and tetramer (in that order). Shoulders to the left and right of the main peak are indicative a slight conformational heterogeneity in the sample, due at least in part to the presence of contaminants. Inset: Coomassie-stained SDS-PAGE gel showing >95% pure TLR11-ECD in the peak fractions. On treatment with endoglycosidase H, the upper bands shift downwards by up to 8 kDa, merging with the lower band. This indicates that the upper bands are TLR11-ECD with different degrees of glycosylation, while the lower band is non-glycosylated protein.

8. Expression and purification of profilin from Toxoplasma gondii

We subcloned the cDNA for Toxoplasma gondii profilin (PFTG) provided by Dr. Sankar Ghosh (Yale School of Medicine) into the pET28b vector (Invitrogen) and transformed it into BL21 E. coli cells. Expression was induced with 0.4 mM IPTG for four hours at 37˚C. Cells were pelleted, lysed by lysozyme treatment and sonication and affinity purified using nickel-NTA agarose beads (Qiagen) and eluted with 0.25 M imidazole in Buffer A (50mM HEPES pH 7, 0.1 M NaCl, 5% glycerol, 2 mM DTT). Nickel-affinity purified protein was dialyzed into Buffer A plus 2 mM calcium chloride. The histidine tag was then cleaved with thrombin and any uncleaved protein was removed with a passage over nickel-NTA agarose beads (Qiagen). Peak fractions were pooled and further fractionated by gel filtration using a Superdex 200 (GE Healthcare) column in 10 mM Tris pH 7.5, 40 mM KCl, 2 mM TCEP (Figure 6).

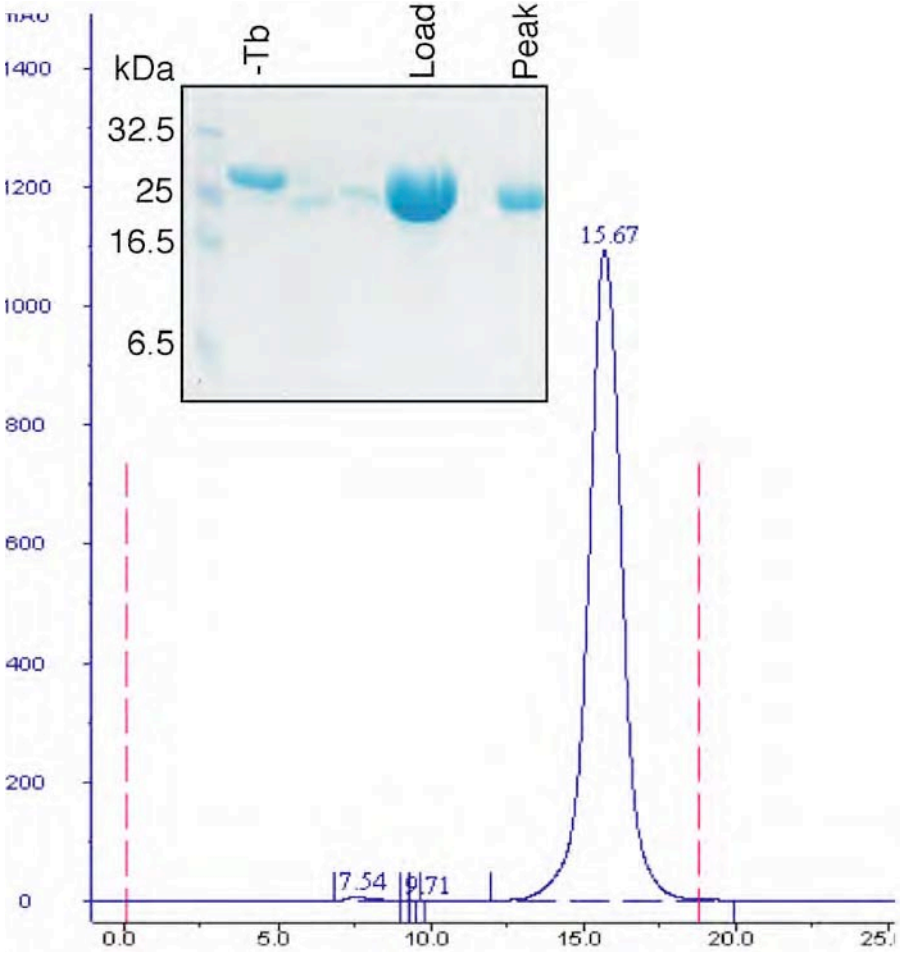

Fig. 6. Size exclusion chromatogram of endogenous profilin from Toxoplasma gondii (PFTG) previously purified by Ni-affinity chromatography. PFTG elutes at 15.67 ml, which corresponds to an apparent size consistent with that of an elongated 18-kDa PFTG monomer. Inset: Coomassie-stained SDS-PAGE gel showing pure PFTG before cleavage of the His6 tag with thrombin (-Tb), prior to loading on the S200 size exclusion column (Load), and in the peak elution fraction from the S200 colum (Peak).

9. Crystallization of profilin from Toxoplasma gondii (PFTG)

With our automated robotic liquid handling system (Hydra II Plus One, Matrix Technologies) we were able to perform crystallization trials on our PFTG material using a large number of custom-made and commercially available precipitant solutions (QIAgen, Hampton Research). We recently obtained small crystals of PFTG (Figure 7). We will use our PFTG crystals to determine the three-dimensional structure of PFTG. The structure determination of PTFG is expected to be straightforward, given the availability of several structures of profilin from other organisms (including human and yeast). A crystal structure of PFTG would greatly assist the structure determination of a TLR11-PFTG complex or a TLR11-TLR12-PFTG complex.

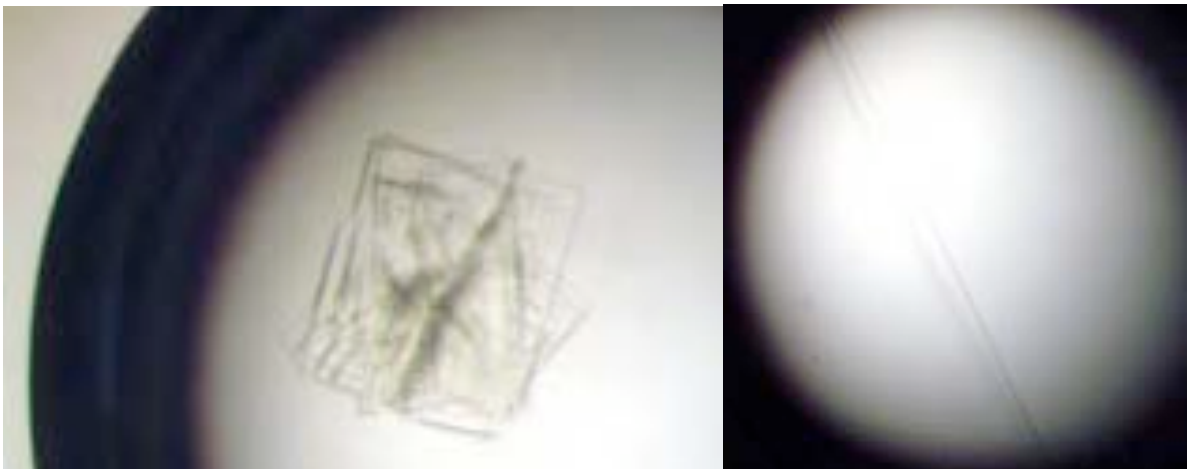

Fig. 7. Crystallization conditions for Toxoplamsa gondii profilin (PFTG). Crystals with either plate-like (left panel) or rod-like (right panel) morphologies were obtained from recombinant PFTG. In order to produce crystals suitable for crystallographic data collection, we are currently optimizing crystallization conditions to minimize clustering of the plates and to increase rod thickness.

10. Crystallographic data collection for PFTG.

We collected a complete crystallographic dataset for PFTG at Argonne National Laboratory on April 16-17, 2008 (Table IV). More recently, we obtained a new crystal form using PFTG material with selenomethionine substituted for methionine. The new crystals diffracted at up to 1.9 Å resolution, at the Argonne National Laboratory in July and August 2008 (data not shown). PFTG has only low sequence identity with yeast and vertebrate profilins (~24%) and is recognized by TLR11 and TLR12. A crystal structure of PFTG would greatly assist the structure determination of a TLR11-TLR12-PFTG complex, which is one of the principal goals of this project. We are currently attempting to determine the structure of PFTG by molecular replacement. Because the method of molecular replacement relies on significant sequence similarity with previously determined structure, however, we will also pursue structure determination of PFTG using the alternative methods of multiple isomorphous replacement (MIR).

Dataset name	**PLVF**
Type of dataset	Native
Space group	$P6_222$
Cell dimensions a , b , c (Å)	105.7, 105.7, 67.4
α , β , γ (˚)	90, 90, 120
Resolution* (Å)	50 – 4.0
R_{merge}*	0.31 (0.76)
I / σI	5.25 (1.52)
Completeness* (%)	95.1 (90.9)
Redundancy*	5.4 (3.6)
Number of molecules per asymmetric unit	1
Solvent content (%)	60

Table IV. Data collection statistics for the native PFTG dataset collected in the current quarter. The dataset was collected on April 16-17, 2008 at Argonne National Laboratory. *Numbers in parentheses refer to the highest resolution shell.

11. Measure the binding affinity of TLR5 for FliC flagellin

Using our purified TLR-ECD material and purified FliC flagellin from Salmonella typhimurium, we have tested for direct binding between the two proteins using several different assays: immunoprecipitation, chemical crosslinking, native gel shift, and size exclusion chromatography. In the immunoprecipitation binding assay, TLR5-ECD was coupled via its histidine tag to nickel-NTA agarose beads. FliC was then passed over the beads, followed by a commercial anti-FliC antibody. The elutate from the nickel beads was then tested by Western blotting for FliC and TLR5-ECD. In the chemical crosslinking assay, FliC and TLR5-ECD were mixed in equimolar ratios and crosslinked with EGS or glutaraldehyde. In the gel shift and size-exclusion chromatography assays, the rate of migration of TLR5-ECD on the gel/column was compared in the presence and absence of FliC. We repeated the binding experiments several times, sometimes varying conditions such as the strain of Salmonella used, the pH, or the length of the TLR5 protein construct (see below).

(a) Immunoprecipitation binding assay. TLR5-ECD was incubated with FliC at 4˚C overnight. A biotinylated anti-pentaHis antibody was then added and the mixture was passed over neutravidin beads (neutravidin binds biotin tightly). The flow-through from the beads, and the beads themselves, were then tested by Western blotting for FliC using anti-FliC antibody (Figure 1). The blot shows that only trace amounts of FliC bind to the beads, regardless of whether TLR5-ECD is present.

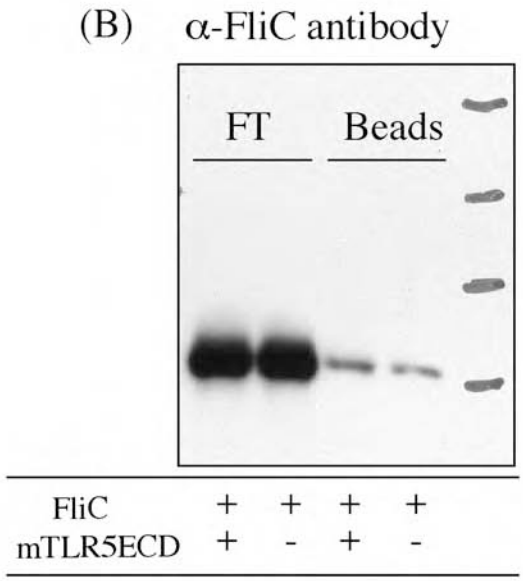

Fig. 8. Immunoprecipitation binding assay of purified TLR5-ECD and FliC. TLR5-ECD was coupled to neutravidin-agarose beads via a biotinylated anti-His5 antibody and the blot was probed with anti-FliC.

(b) Chemical crosslinking assay. FliC and TLR5-ECD were mixed in equimolar ratios and crosslinked with EGS (ethylene glycol bissulfosuccinimidylsuccinate). The crosslinking reaction was then quenched with Tris buffer and analyzed by Western blotting for FliC and TLR5-ECD using anti-FliC and anti-pentahistidine antibodies, respectively (Figure 9). No chemical crosslinking is observed, suggesting that TLR5ECD and FliC do not directly interact without other factors present.

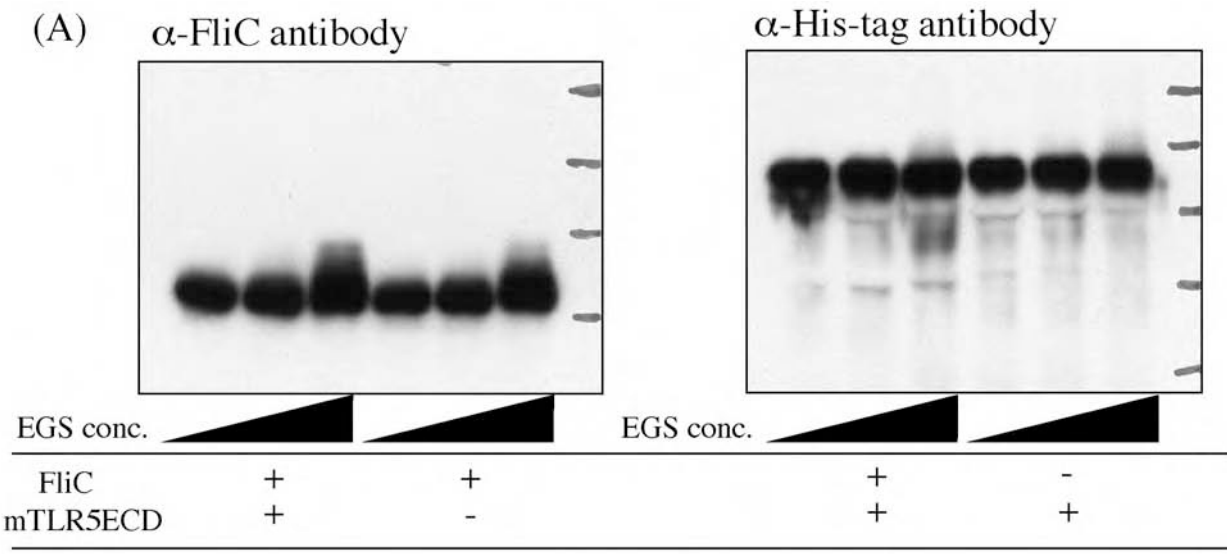

Fig. 9. Chemical crosslinked binding assay of purified TLR5-ECD and FliC. TLR5-ECD was mixed with FliC and 0, 10, 100 μM of the chemical crosslinker EGS was added.

(c) Gel-shift assay. The rate of migration of TLR5-ECD on nondenaturing native PAGE gel was compared in the presence and absence of FliC. The gel was analyzed by Western blotting for FliC and TLR5-ECD using anti-FliC and anti-pentahistidine antibodies, respectively. No significant shift was observed in the rate of migration of the gel bands for FliC and TLR5-ECD (data not shown), suggesting that TLR5-ECD and FliC do not interact directly without additional protein factors.

(d) Size-exclusion chromatography assay. The rate of migration of TLR5-ECD on a Superdex 200 size-exclusion column was compared in the presence and absence of FliC. The eluate from the size-exclusion column was analyzed by Western blotting for FliC and TLR5-ECD using anti-FliC and anti-pentahistidine antibodies, respectively (Figure 10). FliC and TLR5-ECD have the same elution volumes from the size-exclusion column, regardless whether they are run alone or together. This suggests that TLR5-ECD and FliC do not interact directly without additional protein factors.

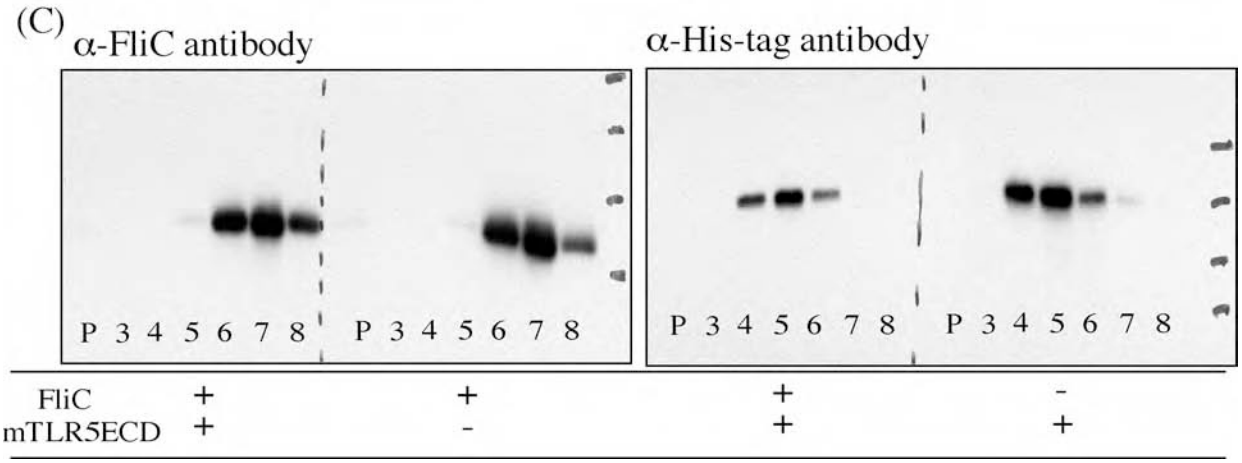

Fig. 10. Size-exclusion chromatography binding assay of purified TLR5-ECD and FliC. TLR5-ECD was mixed with FliC in an equimolar ration and mixture was run on a Superdex 200 size-exclusion column.

Despite several reports in the literature that TLR5 and FliC interact directly (Andersen-Nissen et al., 2007; Smith et al., 2003; Tsujita et al., 2006), all four assays failed to detect direct binding between TLR5-ECD and FliC. We repeated the assays with solubilized full-length human TLR5 instead of mouse TLR5-ECD, and with FliC from a different strain of Salmonella with the same results. We also repeated the assays at a pH of 5.5 to mimic the conditions in an endosome, with still the same results. We conclude that TLR5 requires a co-receptor in order to recognize FliC. Our collaborator Dr. Ghosh's unpublished results suggest that this co-receptor is TLR11. Other TLRs have been previously shown to form heterodimers when they bind their ligands. Specifically, TLR2 forms heterodimers with either TLR1 or TLR6 upon binding bacterial cell wall fragments (Jin et al., 2007).

12. Detection of a complex consisting of TLR5-ECD, TLR11-ECD and FliC formed from purified components

Using our purified TLR5-ECD, TLR11-ECD and FliC, we have begun work to assay for direct binding between the three proteins using various biochemical methods. We now present preliminary evidence that TLR5-ECD, TLR11-ECD and FliC can form a ternary complex in vitro, in the absence of other proteins or cofactors. 20 µg/ml TLR5-ECD, 20 µg/ml TLR11-ECD and 50 µg/ml endogenous FliC from fljB- fliC+ Salmonella typhimurium TH4778 were incubated at 25°C overnight in 0.1 M NaCl, 10 mM triethanolamine pH 7.5, 2 mM foscholine 12, and 50 µg/ml bovine serum albumen (as a blocking agent to reduce non-specific binding or aggregation). In our first assay, the sample and controls were simply subjected to native (nondenaturing) gel electrophoresis. The gel was then analyzed by Western blotting for FliC and TLR5-ECD using anti-FliC and anti-pentahistidine antibodies (QIAgen), respectively. A significant shift was observed in the rate of migration of the gel bands for FliC and TLR5-ECD when TLR5-ECD, TLR11-ECD and FliC were all present (see Figure 11a), suggesting that the three proteins can form a ternary complex in the absence of other factors, and without the TIR signaling domains of the two TLRs. In our second assay, a biotinylated antipentahistidine antibody was added to the sample and the mixture was passed over neutravidin beads (Thermo Fisher Scientific). Bound proteins were then eluted from the beads with SDS-PAGE loading buffer, and the eluates were analyzed by Western blotting using an anti-FliC antibody (Figure 11b). The blot showed that the amount of bound FliC was significantly greater in the presence of both TLR5-ECD and TLR11-ECD. Some residual binding of FliC is observed in the presence of either TLR5-ECD or TLR11-ECD alone. These results demonstrate qualitatively that TLR5-ECD and TLR11-ECD form a complex with FliC in vitro in the absence of other factors. We are currently seeking to confirm and follow up these studies using more quantitative approaches, as described in Research Design and Methods.

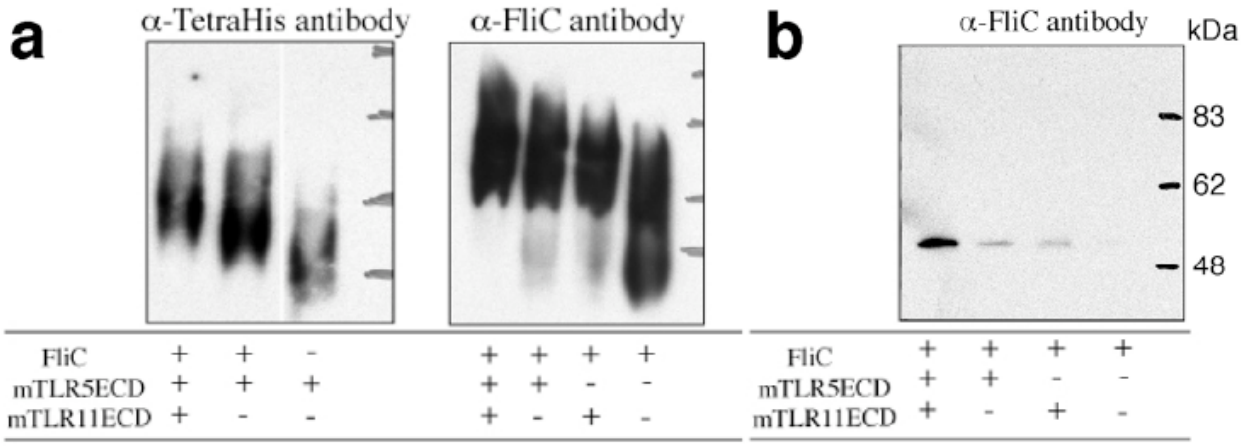

Fig. 11. Detection of a complex consisting of TLR5-ECD, TLR11-ECD and FliC formed from purified components. TLR5-ECD, TLR11-ECD and Salmonella FliC were incubated at 25°C overnight. **(a)** Native gel shift assay. The rate of migration of histidine-tagged TLR5-ECD in nondenaturing PAGE was compared in the presence and absence of FliC and TLR11. A significant shift is observed in the rate of migration of the gel bands for FliC and TLR5-ECD when TLR5-ECD, TLR11-ECD and FliC are all present, suggesting that the three proteins form a ternary complex in the absence of other factors. We note that a smaller shift is observed in the presence of either TLR5-ECD or TLR11-ECD alone, suggesting that each TLR alone has some affinity for FliC. **(b)** Immunoprecipitation binding assay: a biotinylated anti-(His)5 antibody was added and the mixture was passed over neutravidin beads. Proteins that bound to the beads were analyzed by Western blotting with an anti-FliC antibody. The blot shows that the amount of bound FliC is significantly greater in the presence of both TLR5-ECD and TLR11-ECD.

13. Ongoing research

In the original proposal application for this project, the research program was conceived as a three-year program and funded with the understanding that the specific aims would take three years to complete. Our award contract specifies that “Funds may or may not be provided to continue the research in Years 2 and 3”. We are encouraged by the research accomplishments from our first year, described in this report. Based on our current progress, ***we are on track to complete all our objectives— including the structure determination of the TLR5-TLR11-FliC complex and subsequent structure-based vaccine adjuvant design— by the end of our original three-year timeline.*** Our work will guide efforts to design synthetic TLR5/TRL11 agonists, which could serve as novel vaccine adjuvants, or as immunomodulatory therapeutics. Such therapeutics would provide a powerful new means to prevent and treat infectious diseases. ***Therefore, we hope that USAMRMC will consider extending funding to support the second and third years of our research.***

KEY RESEARCH ACCOMPLISHMENTS

- Developed a protocol to purify milligram quantities of TLR5 and TLR11.
- Developed a protocol to purify bacterial flagellin FliC, the ligand for TLR5/TLR11.
- Developed a protocol to purify *Toxoplasma* profilin (PFTG), the ligand for TLR11/TLR12.
- Obtained crystals of TLR5, which diffract to 2.8 Å resolution.
- Collected 18 native crystallographic datasets from TLR5 crystals and 16 potential heavy-metal derivative datasets for use in the structure determination of TLR5.
- Obtained crystals of PFTG, which diffract to 1.9 Å resolution.
- Collected 20 native and derivative crystallographic datasets from PFTG crystals for use in the structure determination of PFTG.
- Showed that purified TLR5 and FliC flagellin do not interact directly with each other in the absence of other proteins or co-factors.
- Obtained the first biochemical evidence that purified TLR5, TLR11 and FliC flagellin interact directly with each other.

REPORTABLE OUTCOMES

As stated in the original proposal application and in the award contract, this project was conceived and funded with the understanding that the specific aims would take three years to complete. We therefore do not yet have any publications, abstracts, or intellectual property to report. Our results for the first year of research did however provide sufficient data for us to apply for an R01 Research Grant from the National Institutes of Health (NIAID grant number 1R01AI082255-01, pending review). Additionally, Dr. Ryuta Kanai, who received pay for research performed for this project, applied for a Postdoctoral Fellowship award from the Japan Society for the Promotion of Science (JSPS), partly on the strength of his results pertaining to this project. JSPS has invited Dr. Kanai for an interview in Japan as part of the second and final round of selection for the fellowship award. Finally, we fully expect our work to be published in leading internationally peer-reviewed journals after the end of our three-year research period.

CONCLUSION

Our key research objective in this project is to obtain the three-dimensional structure of TLR-ligand immune receptor complex. This structure will allow us to formulate a mechanistic hypothesis for the molecular basis of pathogen recognition and proinflammatory signal generation by this important branch of the innate immune system. We will then test our structure-based hypothesis of TLR5/TLR11 function, by measuring the effect on immune signaling of engineered mutations that are predicted to interfere with ligand binding or signal generation. Our structure will also serve as a design platform to seek high-affinity TLR ligands, or agonists. Synthetic TLR agonists could serve as novel vaccine adjuvants, or as immunomodulatory therapeutics. Such therapeutics would provide a powerful new means to prevent and treat infectious diseases.

In the original application for this project, the research program was conceived as a three-year program and funded with the understanding that the proposed research objectives specific aims would take three years to complete. In our first year of research, which is the subject of this report, we reached a number of our stated milestones, making excellent progress towards completing our ultimate goals as stated above. Specifically, while several other research laboratories tried and failed to produce TLRs in the quantities and quality necessary for structural studies, we were able to develop methods to purify milligram quantities of TLR5, TLR11 and two of their ligands FliC and PFTG. We then obtained crystals of TLR5 that diffract to near atomic resolution, and collected over 20 datasets for use in the structure determination of TLR5. We also obtained crystals of PFTG that diffract to 1.9 Å resolution. Crystal structures of TLR5 and PFTG will greatly assist the structure determination of a TLR5-TLR11-flagellin complex or of a TLR11-TLR12-PFTG complex, which is a key goal of this project. In biochemical work, we showed that— despite reports in the literature using crude cell lysate that TLR5 and FliC interact directly (Andersen-Nissen et al., 2007; Smith et al., 2003; Tsujita et al., 2006)— **purified TLR5 and FliC do not interact directly** with each other in the absence of other proteins or co-factors. Furthermore, we obtained the first biochemical evidence that **purified TLR5, TLR11 and FliC flagellin do interact directly with each other**. These are major findings that will change the current paradigm for the signaling mechanism of TLR5. These research accomplishments place us on track to complete all of our objectives by the end of our original three-year timeline. Our award contract specified that *"Funds may or may not be provided to continue the research in Years 2 and 3".* Given our research accomplishments in our first year of funding, we trust that USAMRMC will consider extending funding to support the second and third years of our research program.

REFERENCES

Andersen-Nissen, E., Smith, K.D., Bonneau, R., Strong, R.K. and Aderem, A. (2007) A conserved surface on Toll-like receptor 5 recognizes bacterial flagellin. *J Exp Med*, **204**, 393-403.

Bell, J.K., Botos, I., Hall, P.R., Askins, J., Shiloach, J., Segal, D.M. and Davies, D.R. (2005) The molecular structure of the Toll-like receptor 3 ligand-binding domain. *Proc Natl Acad Sci U S A*, **102**, 10976-10980.

Choe, J., Kelker, M.S. and Wilson, I.A. (2005) Crystal structure of human toll-like receptor 3 (TLR3) ectodomain. *Science*, **309**, 581-585.

Jin, M.S., Kim, S.E., Heo, J.Y., Lee, M.E., Kim, H.M., Paik, S.G., Lee, H. and Lee, J.O. (2007) Crystal structure of the TLR1-TLR2 heterodimer induced by binding of a tri-acylated lipopeptide. *Cell*, **130**, 1071-1082.

Kim, H.M., Park, B.S., Kim, J.I., Kim, S.E., Lee, J., Oh, S.C., Enkhbayar, P., Matsushima, N., Lee, H., Yoo, O.J. and Lee, J.O. (2007) Crystal Structure of the TLR4-MD-2 Complex with Bound Endotoxin Antagonist Eritoran. *Cell*, **130**, 906-917.

Silva-Herzog, E. and Dreyfus, G. (1999) Interaction of FliI, a component of the flagellar export apparatus, with flagellin and hook protein. *Biochim Biophys Acta*, **1431**, 374-383.

Smith, K.D., Andersen-Nissen, E., Hayashi, F., Strobe, K., Bergman, M.A., Barrett, S.L., Cookson, B.T. and Aderem, A. (2003) Toll-like receptor 5 recognizes a conserved site on flagellin required for protofilament formation and bacterial motility. *Nat Immunol*, **4**, 1247-1253.

Tsujita, T., Ishii, A., Tsukada, H., Matsumoto, M., Che, F.S. and Seya, T. (2006) Fish soluble Toll-like receptor (TLR)5 amplifies human TLR5 response via physical binding to flagellin. *Vaccine*, **24**, 2193-2199.

APPENDICES

Publications and Meeting Abstracts

As stated in the original proposal application and in the award contract, this project was conceived and funded with the understanding that the specific aims would take three years to complete. We have no publications or meeting abstracts to report at this stage, after one year of research.

Personnel receiving pay from the research effort

Moshe Dessau, Ph.D.
Ryuta Kanai, Ph.D.
Yorgo Modis, Ph.D.
Christina Newman, M.S.

SUPPORTING DATA

All figures, tables and other supporting data have been embedded in the main body of the report.